Supporting Information

Motion-Based Immunological Detection of Zika Virus Using Pt-Nanomotors and A Cellphone

Mohamed Shehata Draz[1,2,3], Nivethitha Kota Lakshminaraasimulu[1*], Sanchana Krishnakumar[1*], Dheerendranath Battalapalli[1*], Anish Vasan[1*], Manoj Kumar Kanakasabapathy[1], Aparna Sreeram[1], Shantanu Kallakuri[1], Prudhvi Thirumalaraju[1], Yudong Li[1], Stephane Hua[5], Xu G. Yu[4,5], Daniel R. Kuritzkes[4], Hadi Shafiee[1,2]

1. Division of Engineering in Medicine, Department of Medicine, Brigham and Women's Hospital, Harvard Medical School, Boston, MA 02139, USA.

2. Department of Medicine, Harvard Medical School, Boston, USA.

3. Faculty of Science, Tanta University, Tanta 31527, Egypt

4. Division of Infectious Diseases, Brigham and Women's Hospital, Harvard Medical School, Boston, USA.

5. The Ragon Institute of Massachusetts General Hospital, Massachusetts Institute of Technology and Harvard University, Boston, MA 02129

* Authors contributed equally to this work

Corresponding author. Email: hshafiee@bwh.harvard.edu

a. Supporting methods

Uultra violet visible (UV-Vis) Spectroscopy. Absorption spectra were measured on Shimadzu UV-2450 spectrophotometer. The samples were loaded in 10 mm path length quartz cuvettes and scanned at room temperature.

Transmission Electron Microscopy (TEM). TEM images were obtained using a JEOL 2100 TEM microscope at an acceleration voltage of 300 kV. The specimens were prepared by dropping 2 μ l of the sample onto ultrathin Formvar-coated 200-mesh copper grids and then dried in air. The mean diameter and size distribution histogram of particles were obtained by averaging more than 100 particles from the TEM images using ImageJ software.

Scanning electron microscopy (SEM). Supra55VP Field Emission Scanning Electron Microscope (FESEM) instrument operating at 8 kV was used to image the virus particles and formed complex with Pt-nanomotors on the surface of polystyrene beads. After virus capture and assembly with Pt-nanomotors, the beads were washed and deposited on glass slides and sputtered with gold conductive layer for 60 s before SEM imaging experiments were performed.

Fourier transform-infrared (FT-IR) spectroscopy. FT-IR spectra in the region of 4000 cm^{-1} to 500 cm^{-1} were collected in absorbance mode with a resolution of 2 cm^{-1} (FTIR-8400S from Shimadzu, Japan).

Inductively coupled plasma mass spectrometry (ICP-MS). We performed ICP-MS analysis to confirm and evaluate the assembly of virus and Pt-nanomotors on the surface of beads. Standard solutions were prepared by diluting a multi-element standard (1000 mg/L in 1 M HNO_3). Nitric acid (65%), hydrochloric acid (37%), perchloric acid (70%), and hydrogen peroxide (30%) of Suprapur ®grade were used to mineralize the Pt-beads-ZIKV immunocomplexes isolated and washed by centrifugation at 3500 rpm for 10 min. These samples were then digested and purified using size-exclusion column of a HPLC system. The eluted fractions from the HPLC system were detected by ICP-MS (SCIEX ELAN 5000, Perkin Elmer) and Pt concentration was identified using Pt standard.[1,2]

Agarose gel Electrophoresis. The electrophoretic mobility pattern of the prepared Pt-nanomotors compared with non-modified PtNPs was evaluated with a horizontal submerged gel electrophoresis apparatus (Mini-SubCell GT, Bio-Rad) using a 0.5% (w/v) agarose gel in TAE buffer (pH 8.5). 10 μl of sample aliquots were loaded into wells. The gel was subjected to a typical voltage of 100 V for 30 min and imaged with a digital camera.

Quantification of the number of anti-ZIKV mAb per Pt-nanomotors and polystyrene bead. The concentration of monoclonal antibodies (mAbs) was estimated using UV-vis spectroscopy and standard curve prepared from the absorbance of different antibody concentrations at 223 nm. The absorbance value of the antibody was calculated by subtracting the absorbance of control sample (beads or PtNPs) to correct the absorbance background. The number of mAbs per particle was calculated by dividing the

concentration of mAbs by the concentration of the PtNPs or beads. The detailed calculation of the number of mAbs per nanomotor particle can be explained as the following:

The average absorbance value of anti-Zika mAb in nanomotor solution (6.64 pM) is 0.4735. From the standard curve and correlation equation (1) in Figure S6:

$$Y = 0.149 + 0.182\,X \qquad (1)$$

While, Y is the absorbance of mAb at 223 nm and X is the molar concentration of antibody. The concentration of anti-Zika mAb can be calculated to be 0.01189 nM and considering Avogadro's number equal to $6.022140857 \times 10^{23}$, the number of mAb molecules is 0.07160×10^{14}. Similarly, the average number of PtNPs in the nanomotor solution can be estimated to be 0.04×10^{14}. By dividing the number of mAb molecules by the number PtNPs,[3] the average number of mAb per each Pt-nanomotor particle is estimated to be 1.79. Assuming that each mAb labeled with one PDPH molecule carrying one terminal thiol group and each thiol molecule occupies 21. 4 $Å^2$ of the surface of metal nanoparticle, the surface coverage of 1.79 mAb molecule is 38.306 $Å^2$, which represents 6.38% of Pt-nanomotor particle with an average of core diameter of 4.37 nm and surface area of 59.99 nm^2.

SDS gel electrophoresis. To confirm virus capture on beads, protein profiling was performed using SDS-PAGE on 20% Tris-Glycine gel. The beads modified with antibody and captured viruses on beads were digested in digesting buffer and heated for five minutes at 95 ºC on a heat block. For gel electrophoresis analysis, 12 µl of a protein standard and 35 µl of the centrifuged samples were loaded on the gel using a mini-

protean electrophoresis apparatus (Bio-Rad, Hercules, CA). The samples were electrophoresed under 90 V for 50 min. After electrophoresis was done, the gel was rinsed in water for 3 min. Then the gel was stained in the Biosafe Coomassie blue stain for about 1 h. Finally, the gel was de-stained and photographed.

b. Supporting results

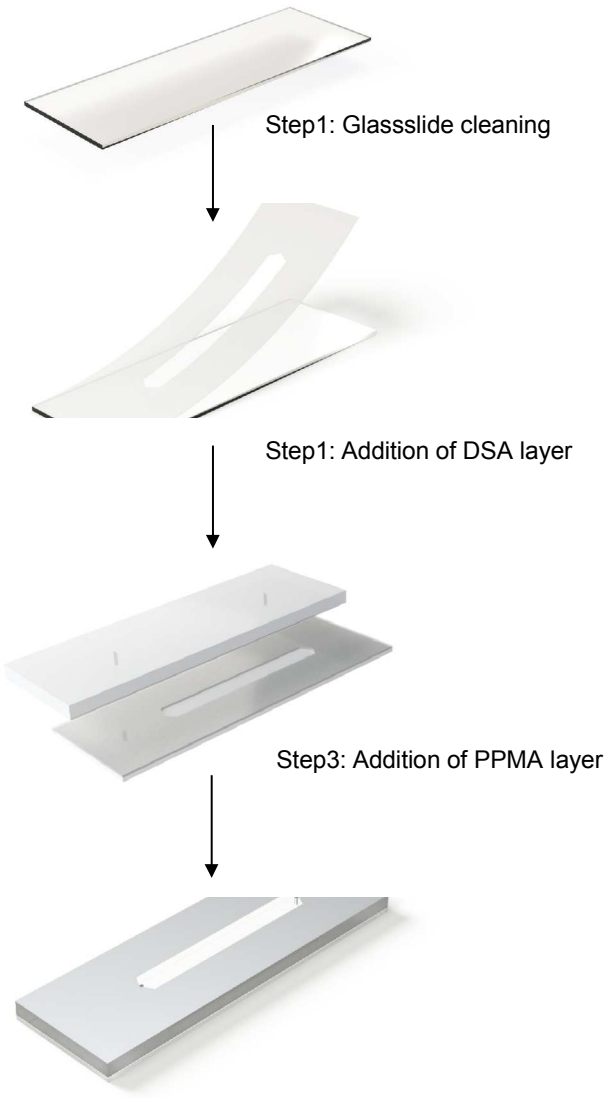

Figure S1. Microchip fabrication protocol

Figure S2. Optical attachment design and detailed structure.

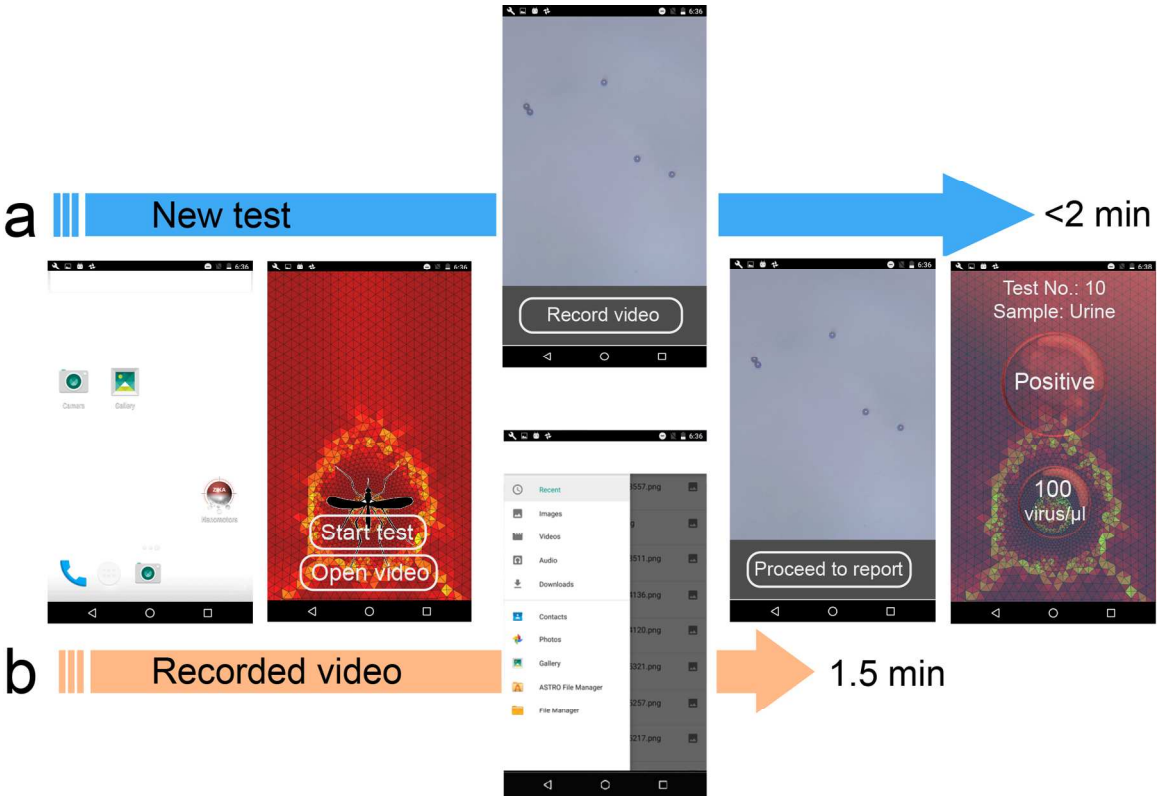

Figure S3. The NBC application flow. The schematic shows the process flow of the Android application used for Zika detection through bead motion change measurement.

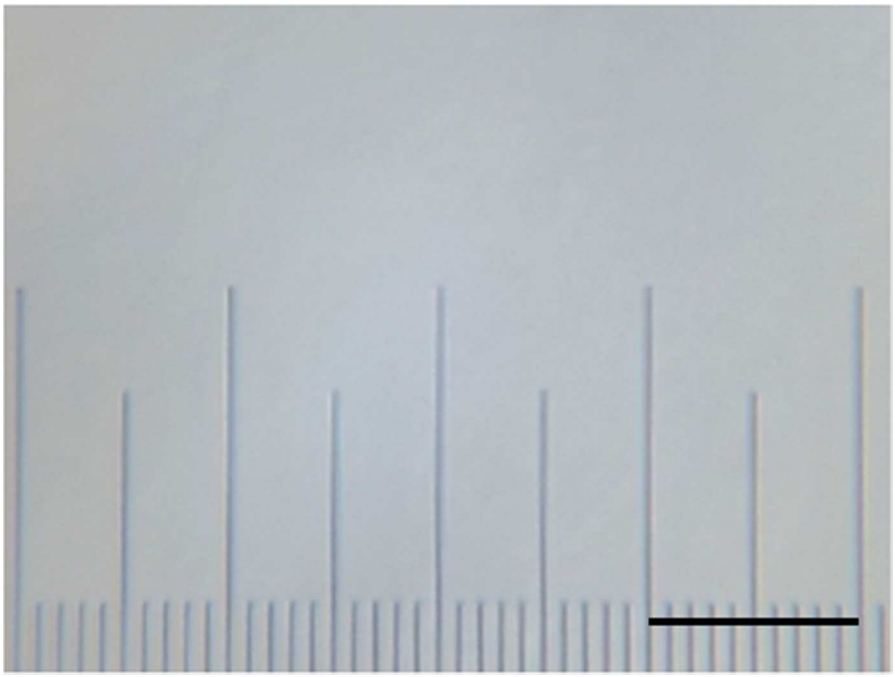

Figure S4. Micrometer scale used for system calibration. Scale bar is 100 μm in size.

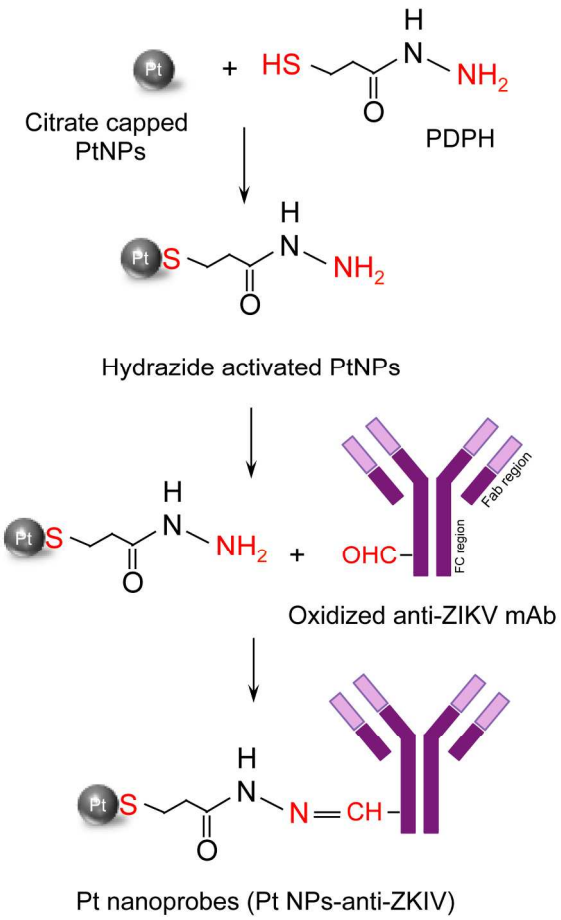

Figure S5. Surface chemistry protocol for antibody conjugation to the surface of PtNPs for Pt-nanomotors preparation. The prepared PtNPs are modified 3-(2-Pyridyldithio)propionyl hydrazide (PDPH) through the thiol binding to the metal surface of PtNPs. The hydrazide terminal of PDPH then reacts with the aldehyde group (CHO) in the oxidized antibody forming the Pt-nanomotors (PtNP-antibody).

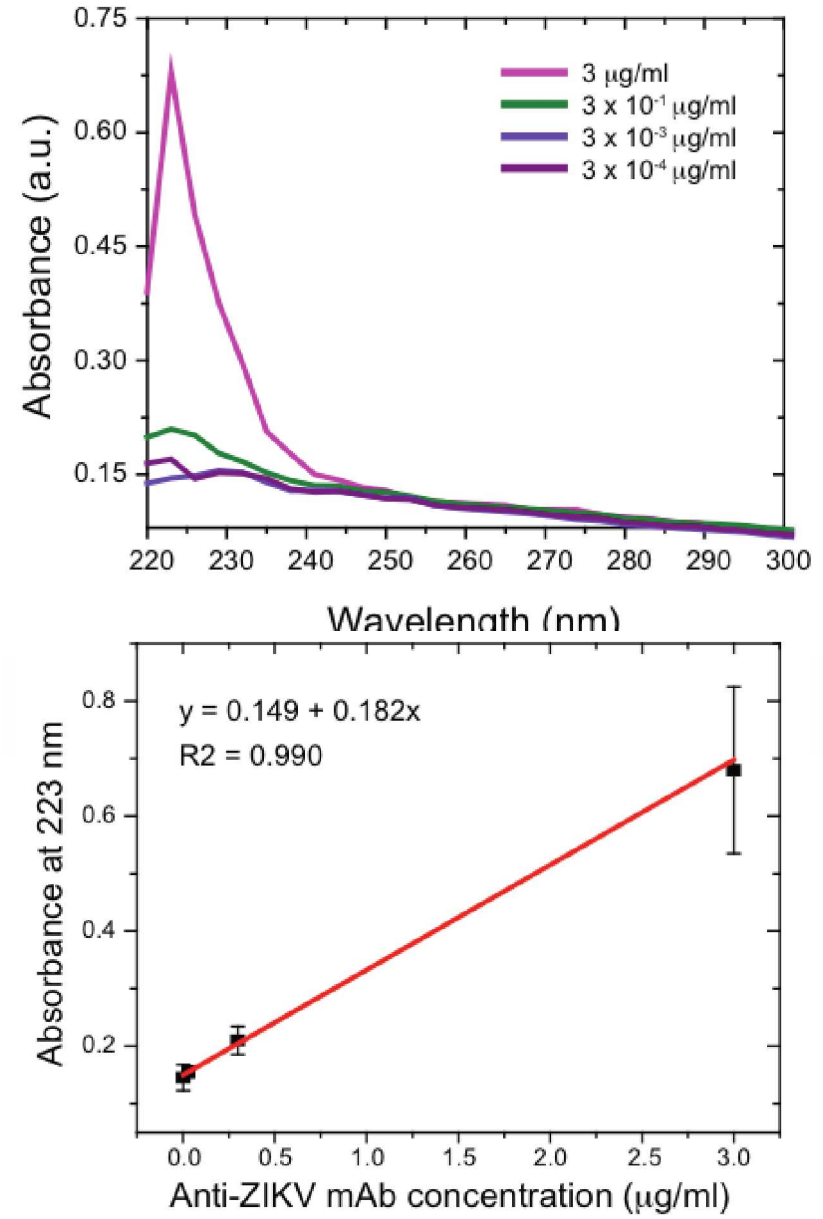

Figure S6. UV-Vis absorbance spectra of different concentrations of anti-ZIKV monoclonal antibody used for the Pt-nanomotor preparation and the corresponding standard curve. Error bars are standard deviations from at least total of three independent measurements.

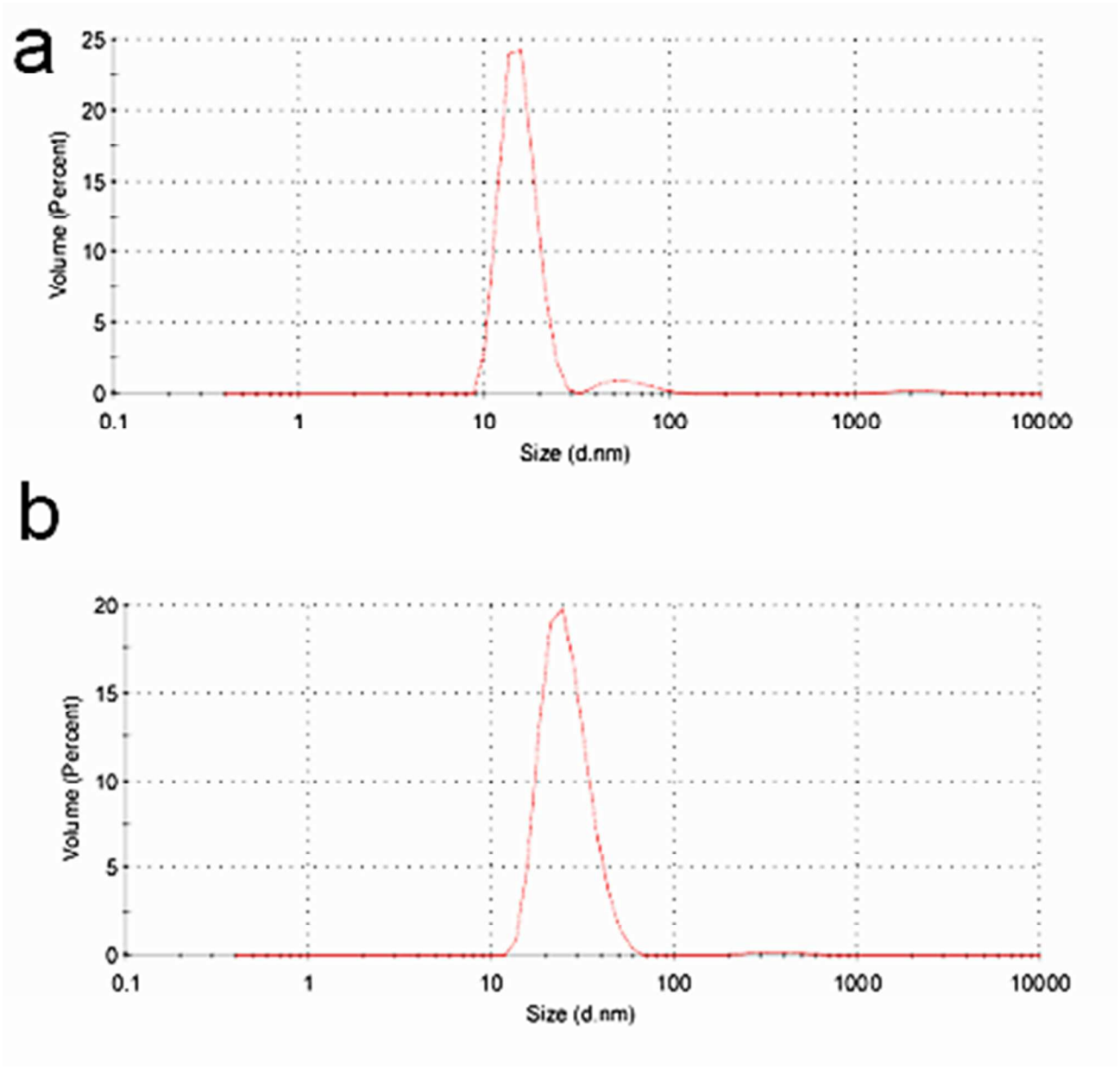

Figure S7. Size analysis using dynamic light scattering technique for (a) PtNPs and (b) Pt-nanomotors with average diameter of 19.375±5.469 nm (n = 3) and 30.456±4.784 nm (n = 3), respectively.

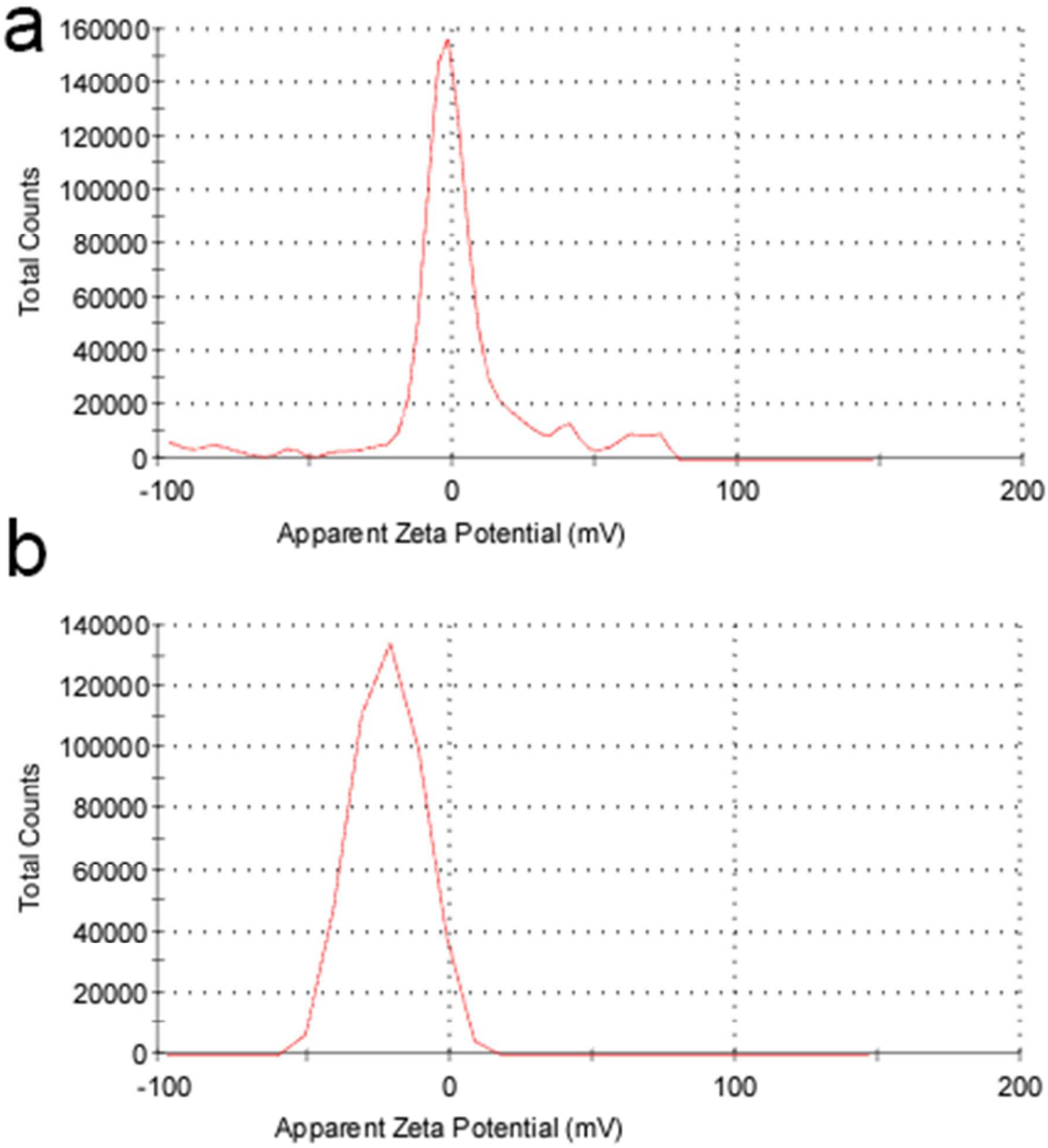

Figure S8. Zeta potential analysis of the surface charge of (a) PtNPs and (b) Pt-nanomotors with values of -9.97±13.75 mV (n = 3) and -18.4±4.9 mV (n = 3), respectively.

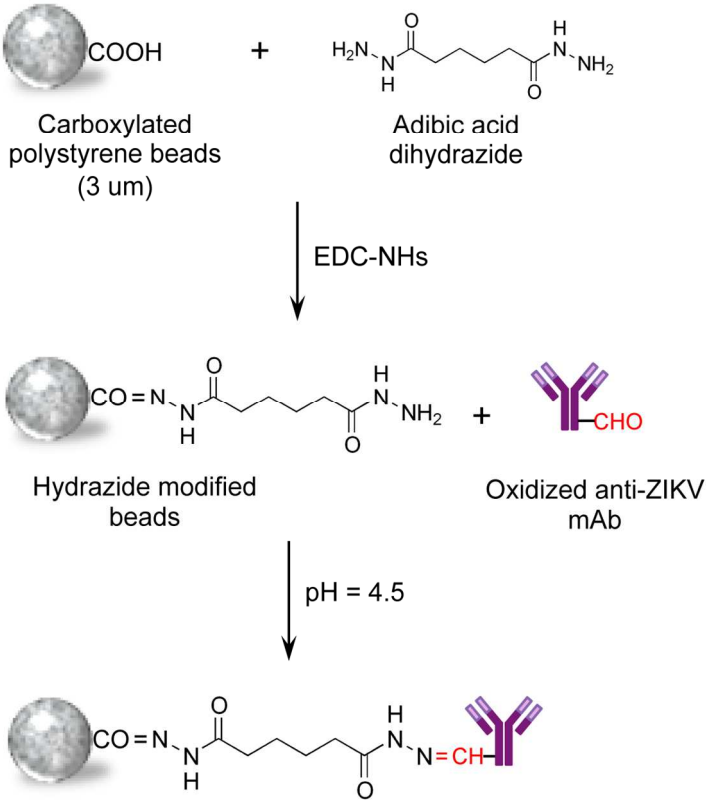

Figure S9. Coupling protocol of antibody to the surface of polystyrene beads. Carboxylated beads are initially activated with adipic acid dihydrazide using 1-ethyl-3-(3-dimethylaminopropyl)carbodiimide hydrochloride(EDC)/N-hydroxysuccinimide (NHS) chemistry. Oxidized anti-Zika virus monoclonal antibody (anti-ZIKV-mAb) with free aldehyde (CHO) group is coupled to the hydrazide-modified beads for ZIKV capturing beads.

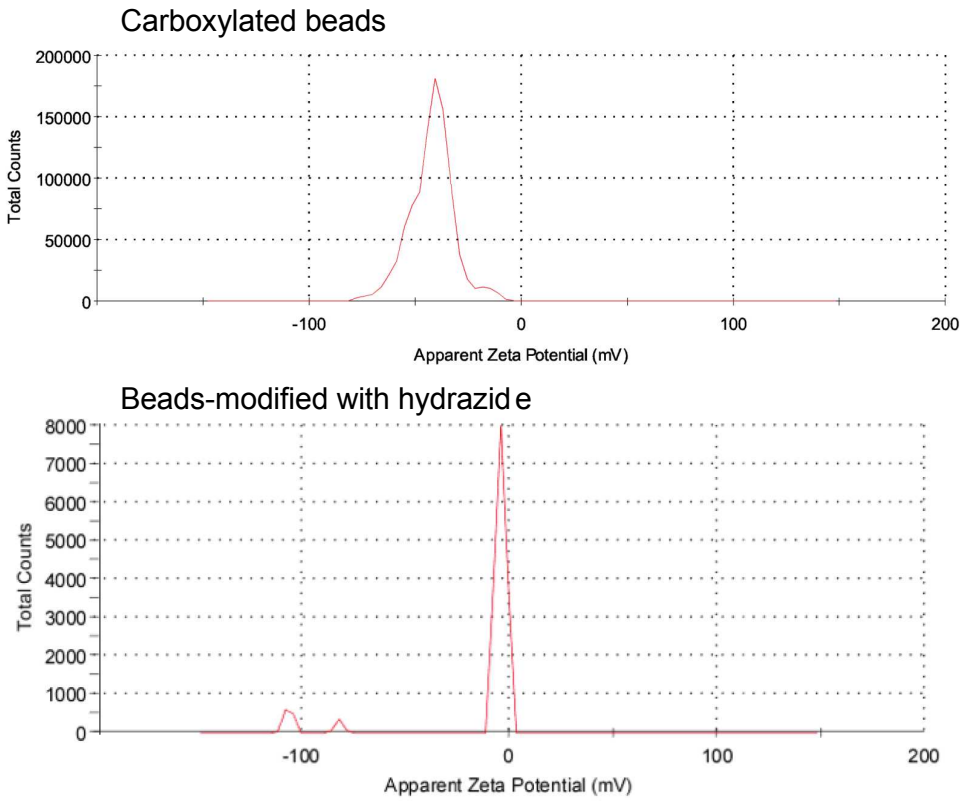

Figure S10. Zeta potential analysis of carboxylated beads and beads modified with adipic dihydrazide.

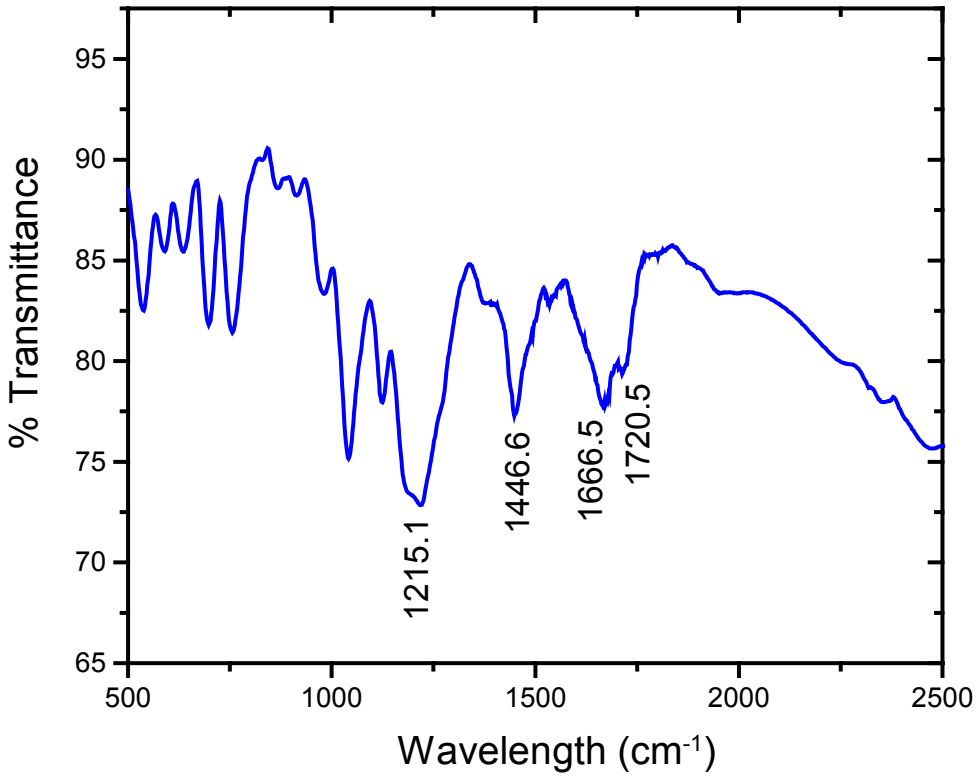

Figure S11. FT-IR of beads with adipic dihydrazide used for coupling with oxidized antibody.

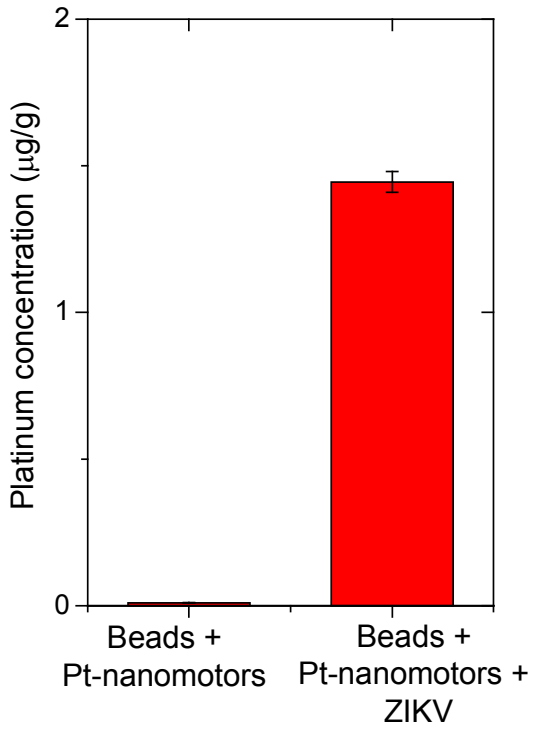

Figure S12. ICP-MS analysis using samples with beads/Pt-nanomotors and beads/Pt-nanomotors/ZIKV complexes. The presence of PtNPs in samples with beads/Pt-nanomotors/ZIKV confirmed the successful capture of ZIKV on motors. Error bars are standard deviations from a total of two to three independent measurements.

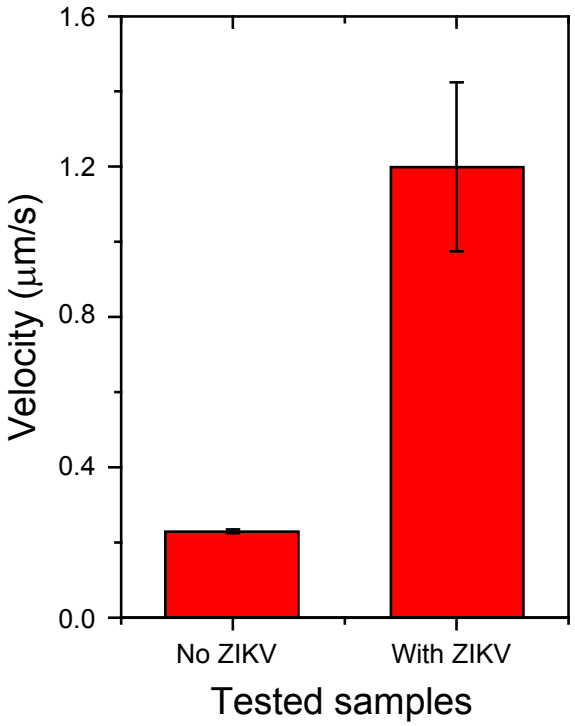

Figure S13. Average motion of beads in the presence and absence of viruses. Error bars are standard deviations from at least total of three independent measurements.

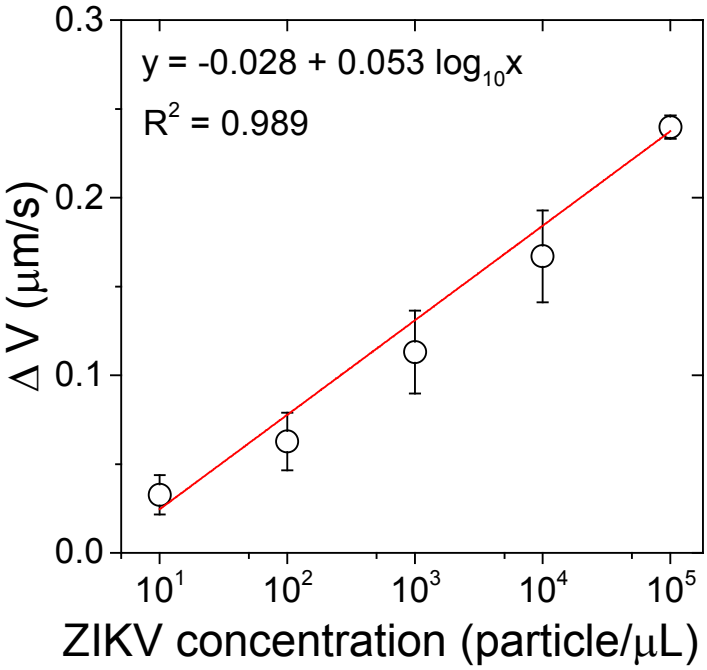

Figure S14. Beads velocity change for samples with different virus concentrations measured using bright-field light microscopy. Error bars are standard deviations from a total of three independent measurements.

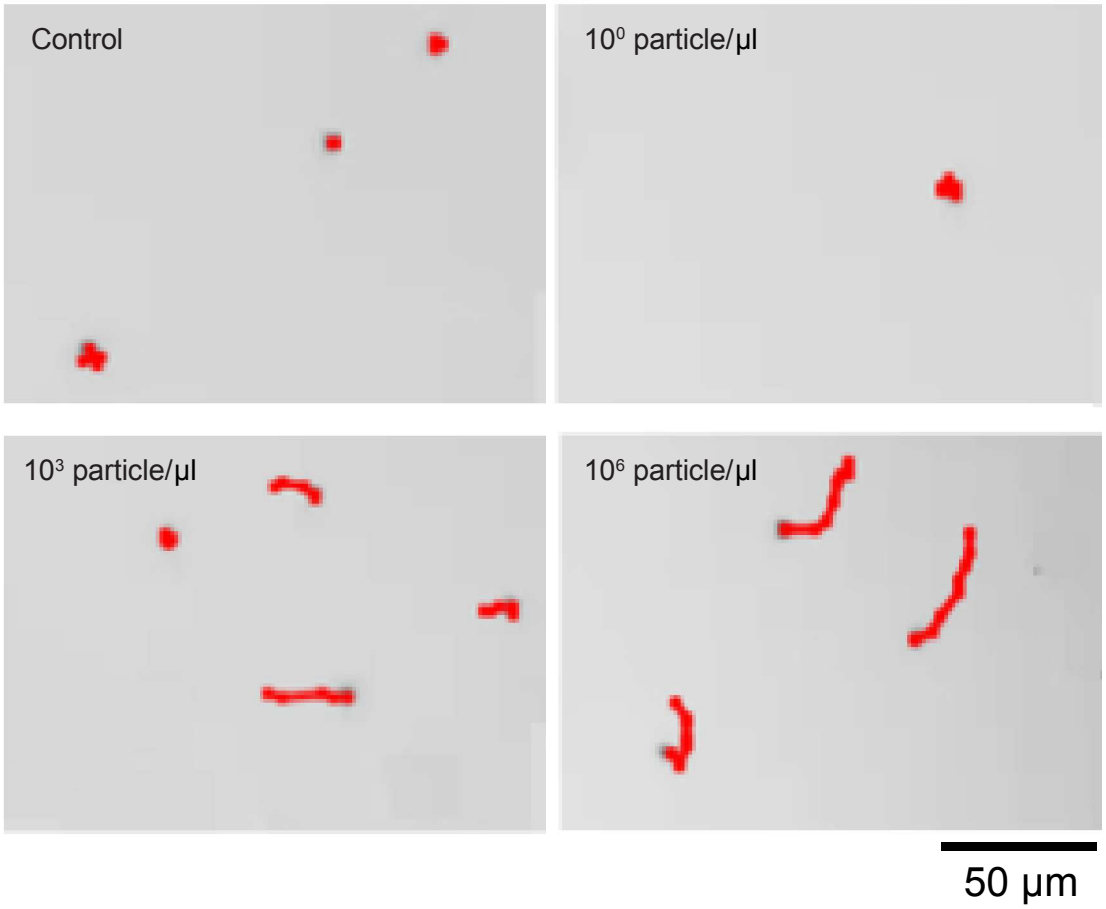

Figure S15. Trajectories of beads motion under bright-field light microscopy in samples with different virus concentrations.

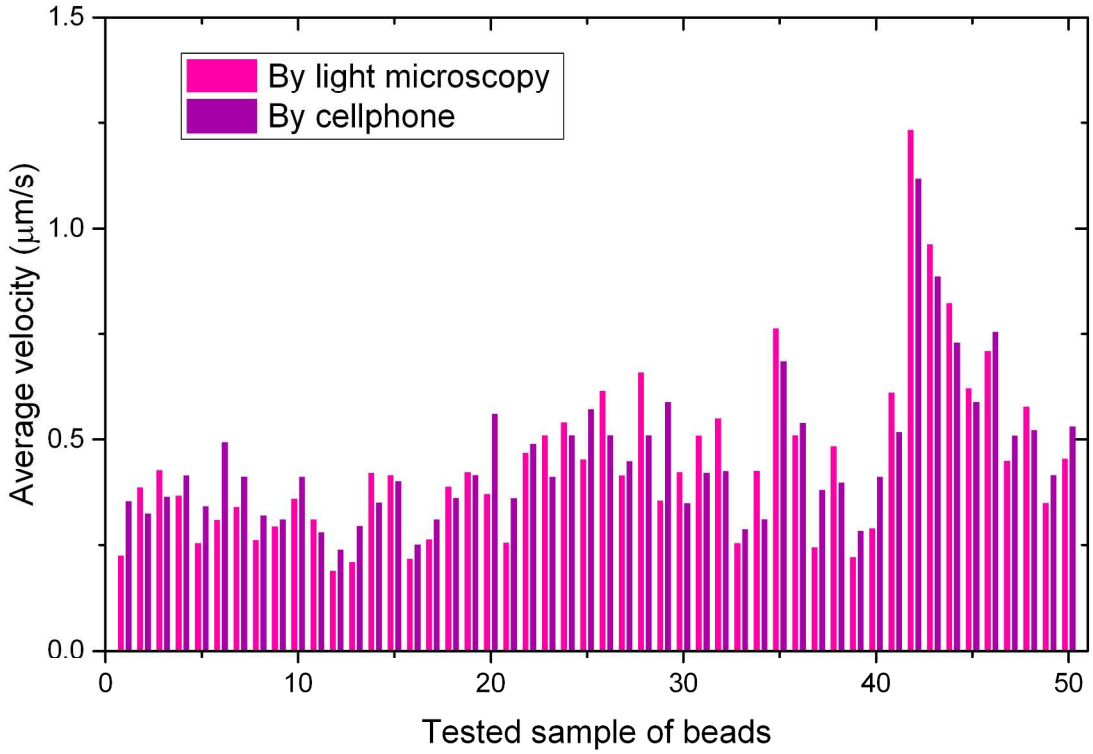

Figure S16. The beads motion measurement results obtained by the NBC system with the smartphone application and a light microscopy using ImageJ software.

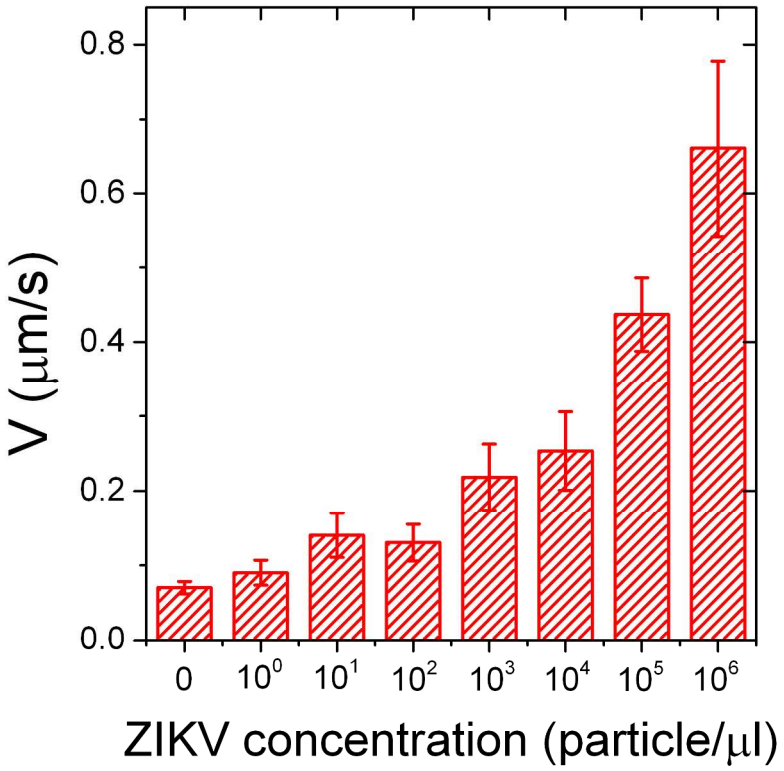

Figure S17. The actual beads velocity magnitudes measured by the NBC for samples with different virus concentrations. Error bars are standard deviations from a total of three independent measurements.

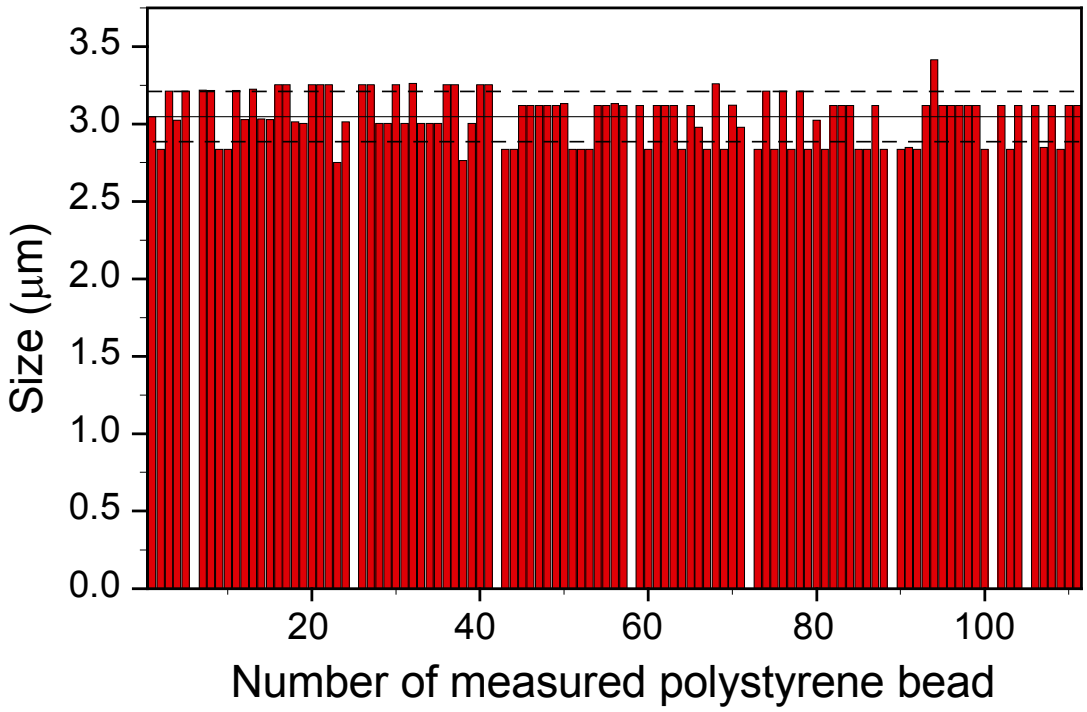

Figure S18. Size variations of the beads used in this study (SD = 0.157 μm).

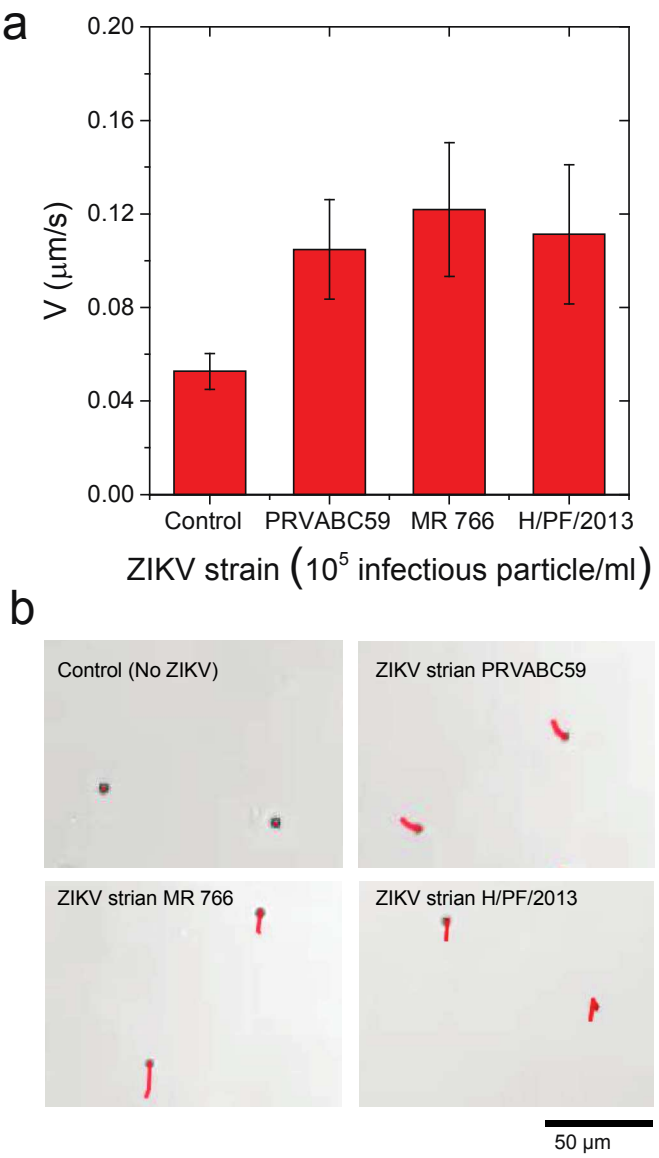

Figure S19. Beads motion in the presence of different ZIKV strains including PRVABC, MR 766, and H/PF/2013. (a) The change in bead motion magnitude with different strains observed by the bright-field light microscopy. (b) Trajectory images of the motion of beads in the presence of different ZIKV strains. Error bars are standard deviations from a total of three independent measurements.

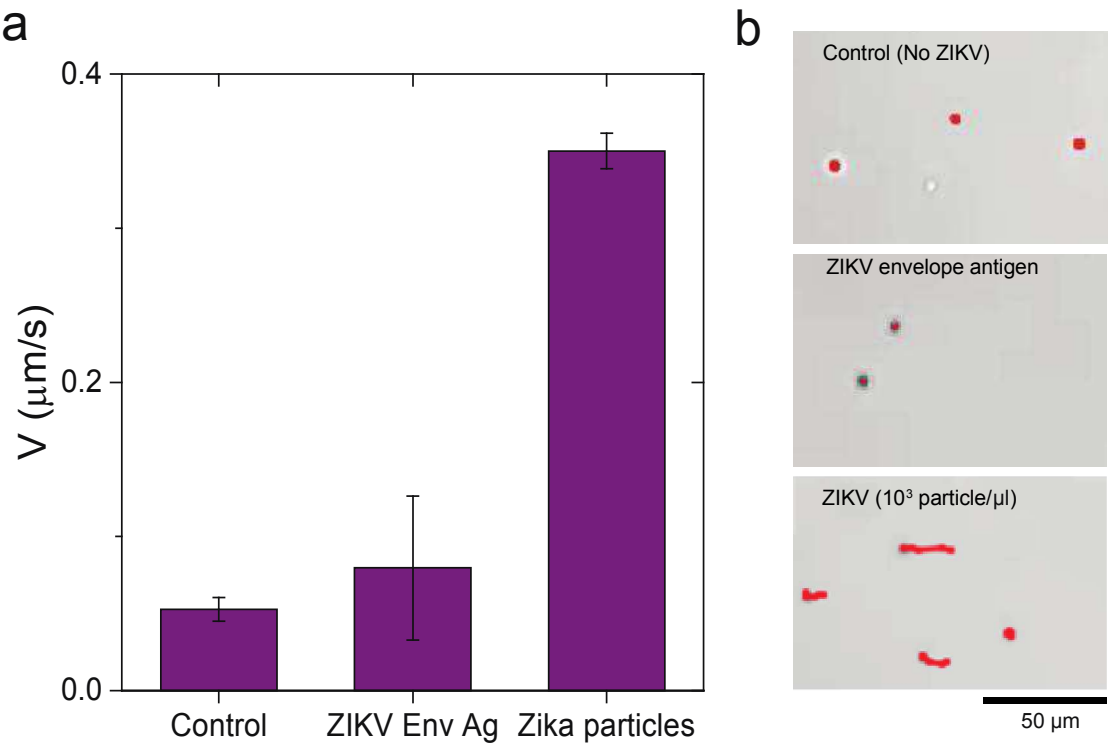

Figure S20. The change in bead motion magnitude in the presence of ZIKV envelope antigen observed by the bright-field light microscopy. Error bars are standard deviations from a total of three independent measurements.

Table S1. Material cost of the 3D printed attachment and the microchip

Item	Cost (USD)	Total
3D printed attachment		3.59
Lenses	1	
Polylactic filament	1.2	
LED	0.09	
Battery	0.6	
Wires and switches	0.7	
Microchips		0.38
PMMA	0.175	
DSA	0.035	
Glass slides	0.17	
		3.97

Supporting movies S1 to S9

Movie S1-ZIKV 0 particle per µl by light microscopy
Movie S2-ZIKV 6 log particles per µl by light microscope
Movie S3-ZIKV 0 particle per µl by light microscopy many
Movie S4-ZIKV 4 log particle by light microscopy many 2
Movie S5-ZIKV 4 log particle by light microscopy many 1
Movie S6-ZIKV 2 log particle per µl by NBC system
Movie S7-ZIKV 4 log particle per µl by NBC system
Movie S8-ZIKV 6 log particle per µl by NBC system
Movie S9-DENV-1 by NBC system

REFERENCES

(1) Drescher, D.; Giesen, C.; Traub, H.; Panne, U.; Kneipp, J.; Jakubowski, N. Quantitative Imaging of Gold and Silver Nanoparticles in Single Eukaryotic Cells by Laser Ablation ICP-MS. *Anal. Chem.* **2012**, *84*, 9684–9688.

(2) Draz, M. S.; Wang, Y.-J.; Chen, F. F.; Xu, Y.; Shafiee, H. Electrically Oscillating Plasmonic Nanoparticles for Enhanced DNA Vaccination against Hepatitis C Virus. *Adv. Funct. Mater.* **2017**, *27*, 1604139.

(3) Ojea-Jiménez, I.; Puntes, V. Instability of Cationic Gold Nanoparticle Bioconjugates: The Role of Citrate Ions. *J. Am. Chem. Soc.* **2009**, *131*, 13320–13327.